

Surface second-order nonlinear optical activity

P. Fischer and A. D. Buckingham

Department of Chemistry, University of Cambridge, Lensfield Road, Cambridge CB2 1EW, UK

Received April 17, 1998; revised manuscript received July 20, 1998

Following the recent observation of a large second-harmonic intensity difference from a monolayer of chiral molecules with left and right circularly polarized light, the scattering theory is generalized and extended to predict linear and circular intensity differences for the more versatile sum-frequency spectroscopy. Estimates indicate that intensity differences should be detectable for a typical experimental arrangement. The second-order nonlinear surface susceptibility tensor is given for different surface point groups in the electric dipole approximation; it is shown that nonlinear optical activity phenomena unambiguously probe molecular chirality only for molecular monolayers that are symmetric about the normal. Other surface symmetries can give rise to intensity differences from monolayers composed of achiral molecules. A water surface is predicted to show linear and nonlinear optical activity in the presence of an electric field parallel to the surface. © 1998 Optical Society of America [S0740-3224(98)01311-3]

OCIS codes: 190.0190, 190.4350, 240.6490.

1. INTRODUCTION

Optical second-harmonic generation (SHG) and sum-frequency generation (SFG) are surface probes and have been extensively used to study a variety of surfaces and interfaces.¹ Both are forbidden in centrosymmetric media under the electric dipole approximation but are allowed at an interface where inversion symmetry is broken.² Two novel optical activity³ phenomena from coherent second-harmonic generation have recently been reported.⁴⁻¹⁴ Hicks *et al.* observed second-harmonic intensity differences from chiral molecules upon reversing the sense of rotation of the incident circularly polarized fundamental, and optical rotation of the second harmonic reflected from a chiral monolayer in linearly polarized light.^{4-8,13} The large SHG circular intensity differences (CID's) were explained in terms of pure electric dipole allowed second-order nonlinear surface susceptibilities $\chi^{(2)}$.^{6,7} The theory has been extended¹⁴ to include magnetic dipole contributions,¹⁰⁻¹² which exist even in isotropic chiral systems. Hecht and Barron¹⁵ discussed optical activity phenomena in linear Rayleigh and Raman scattering from chiral surfaces and alluded that nonlinear analogs of these effects will exist in hyper-Rayleigh, hyper-Raman, SHG, and SFG light scattering. They calculated the Stokes parameters of the surface second-harmonic radiation for arbitrary polarizations for a surface that is symmetric about the normal.¹⁵

The intensity differences in the SHG experiments for chiral molecules are much larger than commonly observed in typical circular-dichroism experiments of linear optics. For example, a monolayer of the *R* enantiomer of 2,2'-dihydroxy-1,1'-binaphthyl (BN) gave a CID of order unity,⁶ while in circular-dichroism experiments the difference between left and right circularly polarized absorptivity divided by their sum is typically $\sim 10^{-3}$.¹⁶ The nonlinear optical activity phenomena, described by $\chi^{(2)}$, are larger in magnitude as the relevant tensor elements of the nonlinear surface susceptibility are dominated by

electric dipole transitions, in contrast to the linear spectroscopies where the rotation and circular dichroism are determined by the rotational strength \mathcal{R} , which is the imaginary part of the scalar product of the electric and magnetic transition dipole moments; \mathcal{R} is nonzero in isotropic chiral media. Barron and Hecht¹⁵ suggest that, since the mechanisms of nonlinear optical activity are distinct from optical activity in linear optics, which are essentially birefringence phenomena, the terms *circular dichroism* and *optical rotatory dispersion* should not be used when describing these nonlinear effects. Further, to avoid confusion, we recommend that *isotropy* should only be applied in three dimensions, and the description 'symmetric about the normal' is appropriate for surfaces or interfaces that are rotationally invariant with respect to the surface normal.

Recently Verbiest *et al.* reported optical activity in SHG experiments from Langmuir-Blodgett films of achiral molecules.¹⁷⁻¹⁹ The nonlinear optical activity experiments using SHG and SFG are probes of molecular chirality only for specific surface symmetries. Surfaces composed of achiral molecules can give rise to nonlinear optical activity phenomena when the experimental arrangement is chiral.¹⁹ We examine here under what conditions different surface symmetries are optically active, and show that nonlinear optical activity phenomena can be observed for all of these surface symmetries using SFG (and most using SHG) even when formed with achiral molecules.

The form of the nonlinearity leading to nonlinear optical activity effects from a surface is reviewed in Section 2. In Section 3 we consider the form of $\chi^{(2)}$ for different surface symmetries and briefly review the basis for the nonlinear optical activity phenomena. In Section 4 we extend the theory to predict similar effects for vibrational SFG and estimate their magnitude. This leads us to predict an experimental arrangement in which water is optically active (Section 5). The conclusions are in Section 6.

2. FORM OF THE SECOND-ORDER NONLINEARITY

The generation of second-harmonic and sum-frequency light at the interface between two centrosymmetric media is described in terms of the induced effective second-order polarization $P_{\text{eff}\alpha}^{(2)}(\Omega)$,²⁰

$$P_{\text{eff}\alpha}^{(2)}(\Omega) = P_{\alpha}^{(2)}(\Omega) - \nabla_{\beta} Q_{\beta\alpha}^{(2)}(\Omega) + \frac{1}{i\Omega} \epsilon_{\alpha\beta\gamma} \nabla_{\beta} M_{\gamma}^{(2)}(\Omega) + \dots, \quad (1)$$

where $P_{\alpha}^{(2)}$, $Q_{\beta\alpha}^{(2)}$, and $M_{\gamma}^{(2)}$ denote the electric dipole density, the electric quadrupole density, and the magnetization, respectively, at the angular frequency Ω .

In this paper we neglect the higher-order contributions in the multipolar expansion of the effective nonlinear polarization and restrict our analysis to the electric dipole contribution that arises from the interfacial layer. The contribution to the signal from the electric quadrupole and magnetic dipole terms in the bulk can be significant,^{21,22} but the dipole part often dominates when the interfacial molecules are ordered²³ and is the only contribution we consider.

The nonlinear optical response from an interface is usually formulated in terms of a surface polarization $P_{S\alpha}^{(2)}$.^{24,25} The dipolar contribution to $P_{S\alpha}^{(2)}$, for monochromatic fields of the form

$$E_{\alpha}(t) = \frac{1}{2} \sum_{\omega \gtrless 0} [E_{\omega\alpha} \exp(-i\omega t) + E_{-\omega\alpha} \exp(i\omega t)], \quad (2)$$

is given by^{26,27}

$$P_{S\alpha}^{(2)}(\Omega) = \epsilon_0 \sum_{\omega} K^{(2)} \chi_{\alpha\beta\gamma}^{(2)} E_{\omega_1\beta} E_{\omega_2\gamma}, \quad (3)$$

where

$$K^{(2)} = \begin{cases} \frac{1}{2} & \text{for second-harmonic generation,} \\ & \text{where } \omega_1 = \omega_2 \\ 1 & \text{for sum-frequency generation} \end{cases}. \quad (4)$$

$\chi_{\alpha\beta\gamma}^{(2)}$ is the nonlinear surface susceptibility tensor, and ϵ_0 is the permittivity of free space. The two incident fields have frequencies ω_1 and ω_2 , and Ω is the sum frequency $\omega_1 + \omega_2$. For a monolayer the nonlinear surface susceptibility $\chi_{\alpha\beta\gamma}^{(2)}$ can be related to the molecular hyperpolarizability tensor $\beta_{ijk}^{(2)}$ (Note 28) through a coordinate transformation from molecule-fixed axes to the frame of the incident radiation α , β , γ averaged over the molecular orientational distribution, denoted below by the angular brackets,

$$\chi_{\alpha\beta\gamma}^{(2)} = \frac{N}{2\epsilon_0} \langle i_{\alpha} j_{\beta} k_{\gamma} \rangle \beta_{ijk}^{(2)}, \quad (5)$$

where summation over i , j , k is implied and N is the number of molecules per unit area.

A relation for the intensity $I_{\sigma}(\Omega)$ of the sum-frequency radiation at Ω in medium σ , originating from an interfacial layer bounded by two bulk isotropic media, $\sigma = 1$ or 2, can be obtained^{24,29}:

$$I_{\sigma}[e_{\alpha}(\Omega), e_{\beta}(\omega_1), e_{\gamma}(\omega_2)] = \frac{\Omega^2 \sec^2 \theta'_i(\Omega)}{2c^3 \epsilon_0 [\epsilon_{\sigma}(\Omega) \epsilon_{\sigma}(\omega_1) \epsilon_{\sigma}(\omega_2)]^{1/2}} \times |e_{\alpha}(\Omega) \chi_{\alpha\beta\gamma}^{(2)} e_{\beta}(\omega_1) e_{\gamma}(\omega_2)|^2 I_{\sigma}(\omega_1) I_{\sigma}(\omega_2), \quad (6)$$

where $e_{\alpha}(\Omega)$, $e_{\beta}(\omega_1)$, and $e_{\gamma}(\omega_2)$ are the Fresnel-corrected polarization vector components for the nonlinear radiation at frequency Ω and for the two incident beams respectively:

$$e_{\alpha}(\Omega) = L_{\alpha\beta}(\Omega) \hat{e}_{\beta\sigma}(\Omega),$$

with $\hat{e}_{\beta\sigma}(\Omega)$, denoting the unit polarization vector of the field at frequency Ω in medium σ and $L_{\alpha\beta}$, the corresponding Fresnel factor, describing the propagation from the bulk σ into the interfacial layer. $I_{\sigma}(\omega_1) I_{\sigma}(\omega_2)$ are the intensities of the pump beams at frequencies ω_1 and ω_2 incident from medium σ . The angle of the radiation at Ω measured from the surface is given by θ'_i , $\epsilon_{\sigma}(\omega_1)$ is the frequency-dependent dielectric constant at ω_1 , etc. We have converted the equation given in Refs. 24 and 29 into SI units. Local field corrections have been ignored.

3. SURFACE SYMMETRIES

In the electric dipole approximation the second-order nonlinear susceptibility is a polar tensor of rank three. Neumann's principle³⁰ states that any type of symmetry exhibited by a particular point group is possessed by every physical property of that system. It follows that a property tensor must transform as the totally symmetric irreducible representation of the system's symmetry group. Birss's tables³¹ of the independent nonvanishing tensor elements can be adapted to show the nonzero tensor components of the second-order nonlinear SFG susceptibility with application to relevant surface symmetries,²⁴ and have since appeared in many different forms, mainly with application to SHG. We distinguish between chiral and achiral susceptibility tensor elements (see Table 1). For SHG the nonlinear susceptibility is symmetric in its last two indices, which reduces the number of independent tensor components further. Should the experimental geometry be rotated with respect to the symmetry axes defined in Table 1, then the components of $\chi^{(2)}$ can be expressed in the rotated frame by invoking a rotation matrix.

We use the convention that the polarization vector for circularly polarized (c.p.) light can be written as $\hat{e}_{\alpha}^{\pm} = (1/\sqrt{2})(\hat{s}_{\alpha} \mp i\hat{p}_{\alpha})$, where the upper sign corresponds to right circular polarization, which is a clockwise rotation of the electric vector when the source is viewed. The electric-field component orthogonal to the plane of incidence lies along the direction of the unit vector $\hat{\mathbf{s}}$, and the parallel-field component lies along the unit vector $\hat{\mathbf{p}}$; the light is propagating in the direction $\hat{\mathbf{s}} \times \hat{\mathbf{p}}$ (see Fig. 1). In a reflection geometry one would commonly find the polarization vectors of an incident beam $I^{(yz)} \hat{\mathbf{e}}^{\pm} = (1/\sqrt{2})[-\hat{\mathbf{x}} \mp i(\hat{\mathbf{y}} \cos \theta + \hat{\mathbf{z}} \sin \theta)]$ and $I^{(xz)} \hat{\mathbf{e}}^{\pm} = (1/\sqrt{2})[\hat{\mathbf{y}} \mp i(\hat{\mathbf{x}} \cos \theta + \hat{\mathbf{z}} \sin \theta)]$, where θ is the angle of incidence (the angle the incident beam makes with the surface normal along $\hat{\mathbf{z}}$ is $\pi - \theta$) and $\hat{\mathbf{z}} = \hat{\mathbf{x}}$

Table 1. Independent Nonvanishing Elements of $\chi^{(2)}(\Omega = \omega_1 + \omega_2)$, the Nonlinear Susceptibility for Sum-Frequency Generation, for Various Surface Symmetries in the Electric Dipole Approximation

Group Symbols Schönflies	Orientation of Symmetry Axes	Nonvanishing Independent Tensor Elements	
		Achiral	Chiral
C_1	any	all 27 elements are nonvanishing and independent	
C_s	$\bar{2}\parallel y$	$xxx, xxz, xzx, xyy, xzz, yxy, yyx,$ $yyz, yzy, zxx, zxz, zzx, zyy, zzz$	-
C_2	$2\parallel z$	$xxz, xzx, yyz, yzy, zxx, zyy, zzz$	$xyz, xzy, yxz, yzx, zxy, zyx$
C_{2v}	$\bar{2}\parallel x, \bar{2}\parallel y$	$xxz, xzx, yyz, yzy, zxx, zyy, zzz$	-
C_3	$3\parallel z$	$xyy = yxy = yyx = -yxy,$ $xyy = yxy = yyx = -xxx, xxz = yzy,$ $xzx = yzy, zxx = zyy, zzz$	$xyz = -yxz, xzy = -yzx, zxy = -zyx$
C_{3v}	$3\parallel z, \bar{2}\parallel y$	$xyy = yxy = yyx = -xxx,$ $xxz = yyz, xzx = yzy, zxx = zyy, zzz$	-
$C_4; C_6; C_\infty$	$4\parallel z; 6\parallel z; \infty\parallel z$	$xxz = yyz, xzx = yzy, zxx = zyy, zzz$	$xyz = -yxz, xzy = -yzx, zxy = -zyx$
$C_{4v}; C_{6v}; C_{\infty v}$	$4\parallel z, \bar{2}\parallel y; 6\parallel z, \bar{2}\parallel y;$ $\infty\parallel z, \bar{2}\perp y$	$xxz = yyz, xzx = yzy, zxx = zyy, zzz$	-

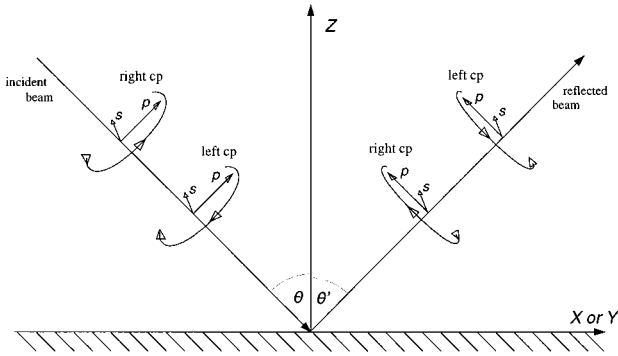


Fig. 1. Beam geometry with left and right c.p. incident and reflected beams.

$\times \hat{y}$. The plane of incidence contains the vectors \hat{y} and \hat{z} for $I^{(yz)}\hat{e}^\pm$ and \hat{x} and \hat{z} for $I^{(xz)}\hat{e}^\pm$; the incident beam makes an angle of $\pi/2 - \theta$ with the y axis or the x axis. Correspondingly the reflected beam can be described by the polarization vectors $R^{(yz)}\hat{e}^\pm = (1/\sqrt{2}) \times [-\hat{x} \mp i(-\hat{y} \cos \theta' + \hat{z} \sin \theta')]$ and $R^{(xz)}\hat{e}^\pm = (1/\sqrt{2})[\hat{y} \mp i(-\hat{x} \cos \theta' + \hat{z} \sin \theta')]$, where θ' is the angle of reflectance (the reflected beam makes an angle of θ' with the surface normal along \hat{z} and an angle of $\pi/2 - \theta'$ with the y axis or the x axis). A linearly polarized input beam with polarization vector \hat{l}_α has its electric-field vector oscillating along either \hat{s} or \hat{p} or a combination of the two. To obtain linear intensity differences (LID's) it is possible to replace right and left circular polarization by linear polarization states at $\pm 45^\circ$ with respect to the plane of incidence, $\hat{l}_\alpha^\pm = (1/\sqrt{2})(\hat{p}_\alpha \pm \hat{s}_\alpha)$, yielding polarization vectors for an incident beam $I^{(yz)}\hat{1}^\pm = (1/\sqrt{2})[(\hat{y} \cos \theta + \hat{z} \sin \theta) \mp \hat{x}]$ and $I^{(xz)}\hat{1}^\pm = (1/\sqrt{2}) \times [(\hat{x} \cos \theta + \hat{z} \sin \theta) \pm \hat{y}]$, and for a reflected beam $R^{(yz)}\hat{1}^\pm = (1/\sqrt{2})[(-\hat{y} \cos \theta' + \hat{z} \sin \theta') \mp \hat{x}]$ and $R^{(xz)}\hat{1}^\pm = (1/\sqrt{2})[(-\hat{x} \cos \theta' + \hat{z} \sin \theta') \pm \hat{y}]$.

Circular and linear intensity differences in SHG arise owing to interferences in the expression for the intensity [see Eq. (6)] between two different nonlinear susceptibility tensor elements. For CID's to be measured, there has

to be more than one susceptibility tensor element in Eq. (6), and at least one has to be complex,^{6,15} i.e., at least one of the frequencies ω_1 , ω_2 , or Ω is near resonance. For example, if the input beam is circularly polarized and a linearly polarized SH signal is detected, then the SHG intensity is given by

$$I(l_\alpha, e_\beta^\pm, e_\gamma^\pm) \propto |l_\alpha \chi_{\alpha\beta\gamma}(s_\beta \mp ip_\beta)(s_\gamma \mp ip_\gamma)|^2 I^2(\omega). \quad (7)$$

The following contributions to I change sign with circularity:

$$\delta I(l_\alpha, e_\beta^\pm, e_\gamma^\pm) \propto (\chi_{lss} - \chi_{lpp})[(\mp) i \chi_{lsp}]^* + \text{c.c.}, \quad (8)$$

where subscripts have been contracted, i.e., $l_\alpha \chi_{\alpha\beta\gamma} s_\beta p_\gamma = \chi_{lsp}$. CID's are given by

$$I^+ - I^- \propto \text{Re}(\chi_{lss} - \chi_{lpp})\text{Im}(\chi_{lsp}) - \text{Im}(\chi_{lss} - \chi_{lpp})\text{Re}(\chi_{lsp}) \propto \text{Im}[(\chi_{lss} - \chi_{lpp})^* \chi_{lsp}], \quad (9)$$

where I^+ and I^- are the total intensities for right and left circularly polarized light, respectively, and where Re denotes the real and Im the imaginary part. These and subsequent expressions for CID's and LID's are completely general and can be applied to different surface symmetries and beam polarizations. For example, the CID's first observed by Hicks and coworkers^{6,13} for a C_∞ surface in a SHG experiment in reflection geometry follow with reference to Table 1:

$$I(s_\alpha, e_\beta^\pm, e_\gamma^\pm) \propto |\chi_{sss} - \chi_{spp}(\mp) 2i\chi_{ssp}|^2 I^2(\omega) \propto |-\chi_{xyz} \cos \theta \sin \theta(\pm) i\chi_{xxz} \sin \theta|^2 \times I^2(\omega), \quad (10)$$

$$I^+ - I^- = d[\text{Re}(\chi_{xyz})\text{Im}(\chi_{xxz}) - \text{Im}(\chi_{xyz})\text{Re}(\chi_{xxz})] \cos \theta \sin^2 \theta, \quad (11)$$

where d is a positive constant, the plane of incidence is the yz plane, and the s -polarized second harmonic is observed.

LID's can be observed even if two or more susceptibility tensors are real¹⁵; for example, if the input beam's linear polarization is at $\pm 45^\circ$ to the plane of incidence, and a SH signal is detected at fixed linear polarization. The SHG intensity

$$I(l_\alpha, l_\beta^\pm, l_\gamma^\pm) \propto |l_\alpha \chi_{\alpha\beta\gamma}(p_\beta \pm s_\beta)(p_\gamma \pm s_\gamma)|^2 I^2(\omega) \quad (14)$$

includes terms that depend on the sign of the input beam's linear polarization:

$$\delta I(l_\alpha, l_\beta^\pm, l_\gamma^\pm) \propto (\chi_{lss} + \chi_{lpp})(l_\pm \chi_{lsp})^* + \text{c.c.} \quad (15)$$

The following LID's can be observed:

$$I^+ - I^- \propto \text{Re}(\chi_{lss} + \chi_{lpp})\text{Re}(\chi_{lsp}) + \text{Im}(\chi_{lss} + \chi_{lpp})\text{Im}(\chi_{lsp}) \quad (16)$$

$$\propto \text{Re}[(\chi_{lss} + \chi_{lpp})^* \chi_{lsp}]. \quad (17)$$

Intensity-difference expressions for SFG (SHG) are examined more systematically in Section 4.

Often one assumes that the surface is symmetric about its normal, giving the C_∞ point group for chiral molecules and $C_{\infty v}$ for achiral molecules. The sample is then characterized by one axis around which it is rotationally invariant, and that lies in the direction of the mean dipole moment.³² Such situations are frequently encountered in adsorbate systems on noncrystalline substrates,^{33,34} and it is generally believed that molecules in floating monolayers are distributed symmetrically about the normal.¹⁸ Indeed most of the reported SH optical activity phenomena were analyzed on the basis of this model.⁴⁻¹⁴ Hecht and Barron¹⁵ have formulated second-harmonic CID's for incident and scattered circular polarization in terms of the appropriate Stokes parameters for surfaces with C_∞ symmetry; they also considered LID's.

4. SUM-FREQUENCY GENERATION AND OPTICAL ACTIVITY

In sum-frequency vibrational spectroscopy, one frequency is usually chosen to lie in the visible, while the other incident frequency may be in the infrared (IR).³⁵ By scanning the infrared frequency, keeping the other frequency fixed, one obtains a vibrational spectrum of the molecules at the interface.²⁴ The technique has been described elsewhere in detail.^{23,35-37}

The SFG intensity is proportional to the magnitude of the effective surface nonlinear susceptibility, $\chi_S^{(2)}(\Omega = \omega_{\text{vis}} + \omega_{\text{IR}})$. It is customary to decompose $\chi_S^{(2)}$ by writing

$$\chi_S^{(2)} = \chi_{\text{NR}}^{(2)} + \chi_{\text{R}}^{(2)}, \quad (18)$$

where $\chi_{\text{R}}^{(2)}$ is the resonant contribution from the surface molecules and $\chi_{\text{NR}}^{(2)}$ is the nonresonant part, which also includes any contributions from the bulk. We restrict our analysis to electric dipole contributions.

A quantum-mechanical expression for the nonlinear susceptibility can be found by use of second-order time-dependent perturbation theory. It is sufficient to retain only two terms when one frequency, usually the infrared ω_{IR} , is near resonance. In that case

$$\chi_{\alpha\beta\gamma}^{(2)}(\Omega = \omega_{\text{vis}} + \omega_{\text{IR}}) \approx \frac{N}{2\epsilon_0} \sum_m \left[\frac{\langle 0|\mu_\alpha|m\rangle\langle m|\mu_\beta|v\rangle}{\hbar(\omega_m - \Omega)} + \frac{\langle 0|\mu_\beta|m\rangle\langle m|\mu_\alpha|v\rangle}{\hbar(\omega_m^* + \omega_{\text{vis}})} \right] \frac{\langle v|\mu_\gamma|0\rangle}{\hbar(\omega_v - \omega_{\text{IR}})}, \quad (19)$$

where $|0\rangle$ is the ground state, $|v\rangle$ is the excited vibrational level of the ground electronic state, and $|m\rangle$ is an excited electronic state whose excitation energy from the ground state is $\hbar\omega_m$. We have used complex transition frequencies between the molecular ground state and the excited states m and v , defined by

$$\omega_v = \omega_v^0 - \frac{i}{2}\Gamma_v, \quad (20)$$

where the real transition frequency is given by ω_v^0 and Γ_v is the full width at half the maximum height of the $i \leftarrow 0$ absorption line; the theory thus embraces damping and is therefore appropriate to near-resonance frequencies. If the sum frequency and the visible beam are far from resonance, it is permissible to use real transition frequencies for Ω and ω_{vis} , and the following complex symmetry relation then approximately holds:

$$\chi_{\alpha\beta\gamma}^*(\Omega = \omega_{\text{vis}} + \omega_{\text{IR}}) \approx \chi_{\beta\alpha\gamma}(\omega_{\text{vis}} = \Omega - \omega_{\text{IR}}) \approx \chi_{\gamma\alpha\beta}(\omega_{\text{IR}} = \Omega - \omega_{\text{vis}}), \quad (21)$$

where the last relation is accurate if ω_{IR} is far from resonance too. The term in brackets in Eq. (19) is the Raman-transition polarizability A_{0v} , and $\langle v|\mu_\gamma|0\rangle$ is the IR transition dipole moment. The mode therefore has to be both IR and Raman active to be observable in resonant sum-frequency spectroscopy.³⁵ Subsequent CID and LID expressions containing antisymmetric Raman-transition polarizability tensor components are likely to be observed only under resonant or preresonant conditions.³⁸

The intensity differences in SFG take a form similar to those in SHG, although now both input beams and the sum-frequency beam could in principle be polarized either linearly, circularly, linearly at $\pm 45^\circ$, or any combination thereof. More susceptibility tensor components can be probed in SFG compared with SHG spectroscopy. If one beam, e.g., the visible, is circularly polarized, then the intensity depending on the sign of the c.p. beam is given by

$$\delta I(l_\alpha, e_\beta^\pm, l_\gamma) \propto (\mp)_{\omega_{\text{vis}}} \text{Im}(\chi_{lsl}\chi_{lpl}^*). \quad (22)$$

If instead either the infrared or the scattered beam is circularly polarized, then similar expressions for the c.p.-sensitive intensity can be found by permuting the order of the beams and their corresponding subscript. For two circularly polarized beams, e.g., both input beams, one finds

$$\begin{aligned} \delta I(l_\alpha, e_\beta^\pm, e_\gamma^\pm) \propto (\mp)_{\omega_{\text{vis}}} & [\text{Im}(\chi_{lss}\chi_{lps}^*) - \text{Im}(\chi_{lsp}^*\chi_{lpp})] \\ & + (\mp)_{\omega_{\text{IR}}} [\text{Im}(\chi_{lss}\chi_{lsp}^*) - \text{Im}(\chi_{lps}^*\chi_{lpp})] \\ & + (\mp)_{\omega_{\text{vis}}} (\mp)_{\omega_{\text{IR}}} [\text{Re}(\chi_{lsp}\chi_{lps}^*) \\ & - \text{Re}(\chi_{lss}\chi_{lpp}^*)]. \end{aligned} \quad (23)$$

In contrast to SHG [single incident beam; see Eq. (10)], Eq. (23) shows that a CID could be detected even if two or more susceptibility tensors are real, and even from

achiral molecules symmetric about the surface normal. The other beam combinations for two c.p. fields can again be found by permutation. The c.p.-sensitive intensity expressions can readily be extended to include three c.p. beams, where one finds 28 c.p.-sensitive terms. The LID's of one beam at $\pm 45^\circ$, e.g., the visible, arise from

$$\delta I(l_\alpha, l_\beta^\pm, l_\gamma) \propto (\pm)_{\omega_{\text{vis}}} \text{Re}(\chi_{lpl}\chi_{lsl}^*), \quad (24)$$

and similarly, for two beams linearly polarized at $\pm 45^\circ$, e.g., the input beams, are due to

$$\begin{aligned} \delta I(l_\alpha, l_\beta^\pm, l_\gamma^\pm) \propto & (\pm)_{\omega_{\text{vis}}} [\text{Re}(\chi_{lpp}\chi_{lsp}^*) + \text{Re}(\chi_{lps}^*\chi_{lss})] \\ & + (\pm)_{\omega_{\text{ir}}} [\text{Re}(\chi_{lpp}\chi_{lps}^*) + \text{Re}(\chi_{lps}^*\chi_{lss})] \\ & + (\pm)_{\omega_{\text{vis}}} (\pm)_{\omega_{\text{ir}}} [\text{Re}(\chi_{lps}\chi_{lsp}^*) \\ & + \text{Re}(\chi_{lpp}^*\chi_{lss})]. \end{aligned} \quad (25)$$

The relation between the macroscopic susceptibility, accessible through experiments, and the appropriate microscopic polarizability [see Eq. (5)] needs to be known to infer anything about molecular properties, such as chirality, from experiment. For C_∞ surface symmetries this relation takes a simple form, such that only achiral hyperpolarizability tensor elements arise in the expressions for the achiral susceptibility tensors, and correspondingly only the achiral elements mix.³² It follows that an observed intensity difference in the C_∞ symmetry group involving a chiral susceptibility tensor can probe molecular chirality for certain polarization combinations. This is, however, no longer true for other surface symmetries, where the relation between the susceptibility tensor and the molecular hyperpolarizability takes a more complicated form. A CID or a LID is then no longer a unique probe of molecular chirality. One can show from Table 1 that achiral molecules in any of the other point groups can give rise to intensity differences. The reported optical activity in SHG experiments from Langmuir-Blodgett films (C_s symmetry) of achiral molecules is such a case.¹⁷⁻¹⁹ Verbiest *et al.*¹⁹ have analyzed the CID's and LID's that can occur in SHG for the symmetries listed in Table 1.

To estimate the magnitude of vibrational SFG intensity differentials, ΔI , defined by

$$\Delta I = \frac{I^+ - I^-}{I^+ + I^-}, \quad (26)$$

using surface vibrational infrared-visible SFG, we consider the degenerate terminal CH_3 vibration of long-chain molecules forming a hypothetical monolayer with C_s surface symmetry.

Hirose *et al.* have simulated CH stretching bands of the methyl group assuming local C_s symmetry for the methyl group.³⁹ The molecular axis system (abc) is defined as shown in Fig. 2. Relations among the vibrationally resonant hyperpolarizability tensor components, $\beta_{\alpha\beta\gamma}^R$, can be estimated with a simple mechanical model^{39,40}:

$$\beta_{aaa}^R = \sqrt{2}\beta_{aca}^R. \quad (27)$$

Further, we assume that the molecular c axis makes an angle ϑ with the surface normal Z and that the a axis of the molecular frame is parallel to the laboratory X axis.

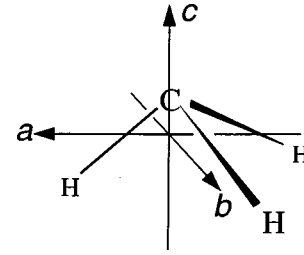


Fig. 2. Molecular coordinate system for CH_3 with C_s symmetry.

The plane of incidence is chosen to be the yz plane, the infrared beam is s polarized, the visible beam's polarization is at $\pm 45^\circ$ to the plane of incidence, and s -polarized SF is detected; then the signal is given by

$$\begin{aligned} I(s_\alpha, l_\beta^\pm, s_\gamma) \propto & |(\pm)\chi_{sss} + \chi_{sps}|^2 I(\omega_{\text{vis}})I(\omega_{\text{ir}}), \\ I^\pm \propto & |(\pm)\chi_{xxx} - \chi_{xxz} \sin \theta_{\text{vis}}|^2 I(\omega_{\text{vis}})I(\omega_{\text{ir}}) \\ & \propto |(\pm)\beta_{aaa} - \beta_{aca} \cos \vartheta \sin \theta_{\text{vis}}|^2 \\ & \times I(\omega_{\text{vis}})I(\omega_{\text{ir}}), \end{aligned} \quad (28)$$

where we ignore Fresnel coefficients. With the relation given in Eq. (27), the intensity differential is given by

$$\Delta I = \frac{-2\sqrt{2} \cos \vartheta \sin \theta_{\text{vis}}}{2 + \cos^2 \vartheta \sin^2 \theta_{\text{vis}}}, \quad (29)$$

which yields $\Delta I \approx 0.77$ for a visible beam incident at 60° and a molecular tilt angle of 40° (corresponds to $\vartheta = 140^\circ$; i.e., the methyl group points away from the surface).

5. OPTICALLY ACTIVE WATER

The structure of water at the liquid-vapor interface can be investigated by x-ray reflection, which can measure the surface roughness and density profiles,^{41,42} whereas SHG on water can in principle measure the distribution of water dipole orientations relative to the surface plane.^{43,44} The interpretation of the SHG experiments is, however, not straightforward,⁴⁴ making infrared-visible sum-frequency generation the preferred technique. Shen and coworkers determined the orientation of water molecules at the water-vapor and quartz-vapor interfaces.^{36,45-47} Their analysis of the infrared-visible SFG vibrational spectra concluded that $\geq 20\%$ of the water molecules at the water-vapor interface have one free OH bond projecting into the vapor and the other hydrogen bonded OH bond pointing into the liquid.⁴⁵

If the molecule possesses a permanent electric dipole moment μ^0 , then the presence of a static electric field \mathbf{E}_0 will exert a torque, $\mu^0 \times \mathbf{E}_0$, on the molecules. The potential energy will vary with the tilt angle θ that the molecules make with the surface normal, the azimuthal angle ϕ , and the electric-field vector:

$$V(\theta, \phi, \mathbf{E}_0) = V(\theta) - \mu_\alpha^0 E_{0\alpha} - 1/2\alpha_{\alpha\beta}^0 E_{0\alpha} E_{0\beta} + \dots, \quad (30)$$

where $\alpha_{\alpha\beta}^0$ is the static polarizability. The average orientation of a molecule in the presence of a field can be found

by taking a Boltzmann average. The appropriate distribution function for the set of Euler angles Ψ is

$$f(\Psi) = \frac{\exp[-V(\theta, \phi, \mathbf{E}_0)/kT]}{\int \exp[-V(\theta, \phi, \mathbf{E}_0)/kT]d\Psi}. \quad (31)$$

The susceptibility tensor is related to the molecular hyperpolarizabilities according to Eq. (5), where the orientational average is now Boltzmann weighted. For weak fields the exponential can be expanded to give

$$\begin{aligned} &\exp[-V(\theta, \phi, \mathbf{E}_0)/kT] \\ &\simeq \exp[-V(\theta)/kT] \left(1 + \frac{\mu_\alpha^0 E_{0\alpha}}{kT} + \dots \right). \end{aligned} \quad (32)$$

An electric field applied parallel to the surface plane would orient the permanent dipole moments of the water molecules such that the surface would then adopt a C_s symmetry configuration, which can give rise to nonlinear optical activity phenomena such as CID's and LID's.

6. CONCLUSIONS

In this paper we have extended the theory of second-harmonic optical activity and have described related experimental options for SFG spectroscopy. We have developed a general formalism of surface nonlinear optical activity in the electric dipole approximation, applicable to various surface symmetries. Depending on the beam polarizations, CID's and LID's could be observable in SFG spectroscopy for all of the surface symmetries listed in Table 1. An intensity-difference signal is only a probe of molecular chirality for surface symmetries where the molecular distribution function is known to be symmetrical about the normal (C_∞ symmetry) and again only for certain polarization combinations. For the general case this is no longer true, and CID's and LID's can be observed for achiral molecules in various conformations. Intensity differences in resonant SFG spectroscopy should be detectable in a standard experimental arrangement with a typical surface coverage N . The results of this paper should be useful in applications of SHG and especially SFG to the study of interfaces with different symmetries. It puts the potential of the second-order techniques as a probe of molecular chirality into perspective. A topical application of SFG optical activity is in the study of water at the liquid/vapor interface. We have proposed an optically active conformation for water in a static electric field parallel to the surface.

ACKNOWLEDGMENTS

P. Fischer gratefully acknowledges the award of a Research Studentship by the Engineering and Physical Sciences Research Council.

REFERENCES AND NOTES

1. Y. R. Shen, *The Principles of Nonlinear Optics* (Wiley, New York, 1984).
2. The nonlinear bulk susceptibility $X^{(2)}$ does not vanish for a chiral liquid in SFG spectroscopy. It has an isotropic chirally sensitive component, $\epsilon_{\alpha\beta\gamma}X^{(2)}$, where $X^{(2)} = 1/6\epsilon_{\alpha\beta\gamma}X_{\alpha\beta\gamma}^{(2)}$. See P. M. Rentzepis, J. A. Giordmaine, and K. W. Wecht, "Coherent optical mixing in optically active liquids," *Phys. Rev. Lett.* **16**, 792 (1966).
3. The differential scattering of right and left circularly polarized light. Nonlinear optical activity is observed in nonlinear light scattering, such as SFG.
4. H. I. Yee, J. D. Byers, T. Petralli-Mallow, and J. Hicks, "Laser techniques for state-selected and state-to-state chemistry," *Proc. SPIE* **1858**, 343 (1993).
5. T. Petralli-Mallow, T. M. Wong, J. D. Byers, H. I. Yee, and J. Hicks, "Circular-dichroism spectroscopy at interfaces: a surface 2nd harmonic-generation study," *J. Phys. Chem.* **97**, 1383 (1993).
6. J. D. Byers, H. I. Yee, T. Petralli-Mallow, and J. Hicks, "Second-harmonic generation circular-dichroism spectroscopy from chiral monolayers," *Phys. Rev. B* **49**, 14 643 (1994).
7. H. I. Yee, J. D. Byers, and J. Hicks, "Laser techniques for surface science," *Proc. SPIE* **2125**, 119 (1994).
8. J. D. Byers, H. I. Yee, and J. Hicks, "A 2nd-harmonic generation analog of optical-rotatory dispersion for the study of chiral monolayers," *J. Chem. Phys.* **101**, 6233 (1994).
9. M. J. Crawford, S. Haslam, J. M. Probert, Y. A. Gruzdkov, and J. G. Frey, "Second harmonic generation from the air/water interface of an aqueous solution of the dipeptide Boc-Trp-Trp," *Chem. Phys. Lett.* **229**, 260 (1994).
10. T. Verbiest, M. Kauranen, A. Persoons, M. Ikonen, J. Kurkela, and H. Lemmetyinen, "Nonlinear-optical activity and biomolecular chirality," *J. Am. Chem. Soc.* **116**, 9203 (1994).
11. M. Kauranen, T. Verbiest, J. J. Maki, and A. Persoons, "2nd-harmonic generation from chiral surfaces," *J. Chem. Phys.* **101**, 8193 (1994).
12. M. Kauranen, T. Verbiest, E. W. Meijer, E. E. Havinga, M. N. Teerenstra, A. J. Schouten, R. J. M. Nolte, and A. Persoons, "Chiral effects in the 2nd-order optical nonlinearity of a poly(isocyanide) monolayer," *Adv. Mater.* **7**, 641 (1995).
13. J. Hicks, T. Petralli-Mallow, and J. D. Byers, "Consequences of chirality in second-order non-linear spectroscopy at surfaces," *Faraday Discuss. Chem. Soc.* **99**, 341 (1994).
14. J. J. Maki, M. Kauranen, and A. Persoons, "Surface second-harmonic generation from chiral materials," *Phys. Rev. B* **51**, 1425 (1995).
15. L. Hecht and L. D. Barron, "New aspects of second-harmonic optical activity from chiral surfaces and interfaces," *Mol. Phys.* **89**, 61 (1996).
16. T. M. Lowry, *Optical Rotatory Power*, reprint ed. (Dover, New York, 1964).
17. T. Verbiest, M. Kauranen, Y. V. Rompanaey, and A. Persoons, "Optical activity of anisotropic achiral surfaces," *Phys. Rev. Lett.* **77**, 1456 (1996).
18. T. Verbiest, Y. V. Rompanaey, M. Kauranen, and A. Persoons, "Anisotropic floating monolayers of 2-docosylamino-5-nitropyridine studied by second-harmonic generation," *Chem. Phys. Lett.* **257**, 285 (1996).
19. T. Verbiest, M. Kauranen, and A. Persoons, "Optical activity of anisotropic achiral surfaces," *J. Opt. Soc. Am. B* **15**, 451 (1998).
20. P. S. Pershan, "Nonlinear optical properties of solids: energy considerations," *Phys. Rev.* **130**, 919 (1963).
21. P. Guyot-Sionnest and Y. R. Shen, "Local and nonlocal surface nonlinearities for surface optical second-harmonic generation," *Phys. Rev. B* **35**, 4420 (1987).
22. P. Guyot-Sionnest and Y. R. Shen, "Bulk contribution in surface second-harmonic generation," *Phys. Rev. B* **38**, 7985 (1988).
23. K. B. Eisenthal, "Liquid interfaces probed by second-harmonic and sum-frequency spectroscopy," *Chem. Rev.* **96**, 1343 (1996).
24. T. F. Heinz, "Second-order nonlinear optical effects at surfaces and interfaces," in *Nonlinear Surface Electromagnetic Phenomena*, H. E. Ponath and G. I. Stegman, eds. (Elsevier, Amsterdam, 1991), p. 353.

25. J. E. Sipe, "New Green-function formalism for surface optics," *J. Opt. Soc. Am. B* **4**, 481 (1987).
26. P. N. Butcher and D. Cotter, *The Elements of Nonlinear Optics*, Vol. 9 of Cambridge Studies in Modern Optics, reprint ed. (Cambridge U. Press, Cambridge, UK, 1993).
27. J. F. Ward and G. H. C. New, *Phys. Rev.* **185**, 57 (1969).
28. The total dipole moment of the molecule is given by $\mu_a = \mu_a^{(0)} + \alpha_{\alpha\beta} E_\alpha + 1/2\beta_{\alpha\beta\gamma} E_\beta E_\gamma + \dots$, where $\mu_a^{(0)}$ is the permanent dipole moment. See A. D. Buckingham and J. A. Pople, "Theoretical studies of the Kerr effect. I. Deviations from a linear polarization law," *Proc. Phys. Soc. London, Sect. A* **68**, 905 (1955).
29. V. Mizrahi and J. E. Sipe, "Phenomenological treatment of surface second-harmonic generation," *J. Opt. Soc. Am. B* **5**, 660 (1988).
30. F. E. Neumann, *Vorlesungen über die Theorie der Elastizität der festen Körper und des Lichtäthers* (Teubner, Leipzig, 1855).
31. R. R. Birss, *Symmetry and Magnetism*, 2nd ed., Vol. 3 of Selected Topics in Solid State Physics (North-Holland, Amsterdam, 1964).
32. B. Dick, "Irreducible tensor analysis of sum- and difference-frequency generation in partially ordered samples," *Chem. Phys.* **96**, 199 (1985).
33. T. F. Heinz, C. K. Chen, D. Ricard, and Y. R. Shen, "Spectroscopy of molecular monolayers by resonant 2nd-harmonic generation," *Phys. Rev. Lett.* **48**, 478 (1982).
34. T. F. Heinz, C. K. Chen, and Y. R. Shen, "Determination of molecular orientation of monolayer adsorbates by optical second-harmonic generation," *Phys. Rev. A* **28**, 1883 (1983).
35. C. D. Bain, "Sum-frequency vibrational spectroscopy of the solid/liquid interface," *J. Chem. Soc., Faraday Trans.* **91**, 1281 (1995).
36. P. Guyot-Sionnest, J. H. Hunt, and Y. R. Shen, "Sum-frequency vibrational spectroscopy of a Langmuir film: study of molecular orientation of a two-dimensional system," *Phys. Rev. Lett.* **59**, 1597 (1987).
37. X. D. Zhu, H. Suhr, and Y. R. Shen, "Surface vibrational spectroscopy by infrared-visible sum frequency generation," *Phys. Rev. B* **35**, 3047 (1987).
38. L. Hecht and L. D. Barron, "Rayleigh and Raman optical activity from chiral surfaces," *Chem. Phys. Lett.* **225**, 525 (1994).
39. C. Hirose, H. Yamamoto, N. Akamatsu, and K. Domen, "Orientation analysis by simulation of vibrational sum-frequency generation spectrum: CH stretching bands of the methyl group," *J. Phys. Chem.* **97**, 10 064 (1993).
40. C. Hirose, N. Akamatsu, and K. Domen, "Formulas for the analysis of the surface sum-frequency generation spectrum by CH stretching modes of methyl and methylene groups," *J. Chem. Phys.* **96**, 997 (1991).
41. A. Braslau, M. Deutsch, P. S. Pershan, A. H. Weiss, L. Alsnien, and J. Bohr, "Surface-roughness of water measured by x-ray reflectivity," *Phys. Rev. Lett.* **54**, 114 (1985).
42. A. Braslau, P. S. Pershan, G. Swislow, B. M. Ocko, and J. Alsnien, "Capillary waves on the surface of simple liquids measured by x-ray reflectivity," *Phys. Rev. A* **38**, 2457 (1988).
43. B. Yang, D. E. Sullivan, B. Tjijto-Margo, and C. G. Gray, "Molecular orientational structure of the water liquid vapor interface," *J. Phys.: Condens. Matter* **3**, 109 (1991).
44. M. C. Goh, J. M. Hicks, K. Kemnitz, G. R. Pinto, K. Bhattacharyya, K. B. Eisenthal, and T. F. Heinz, "Absolute orientation of water-molecules at the neat water-surface," *J. Phys. Chem.* **92**, 5074 (1988).
45. Q. Du, R. Superfine, E. Freysz, and Y. R. Shen, "Vibrational spectroscopy of water at the vapor water interface," *Phys. Rev. Lett.* **70**, 2313 (1993).
46. P. Guyot-Sionnest, R. Superfine, J. H. Hunt, and Y. R. Shen, "Vibrational spectroscopy of a silane monolayer at air solid and liquid solid interfaces using sum-frequency generation," *Chin. Phys. Lasers* **144**, 1 (1988).
47. Q. Du, E. Freysz, and Y. R. Shen, "Surface vibrational spectroscopy of water-molecules at interfaces," *Science* **264**, 826 (1994).